Chemical characteristics and environmental drivers of nitrogen-containing organic aerosol formation in coastal and inland urban atmospheres in Myanmar

Ning Zhang[1,2], Jialiang Feng[2], Simon Patrick O'Meara[3,4], Ziyi Liu[5], Yingge Ma[6,7], Xinlei Ge[8], Wenjing Li[9], Piero Chiacchiaretta[10,11], Piero Di Carlo[10,11], Junfeng Wang[1*], Eleonora Aruffo[11,12]

1. Jiangsu Key Laboratory of Atmospheric Environment Monitoring and Pollution Control (AEMPC), Collaborative Innovation Center of Atmospheric Environment and Equipment Technology (CIC-AEET), School of Environmental Science and Engineering, Nanjing University of Information Science and Technology, Nanjing 210044, China
2. School of Environmental and Chemical Engineering, Shanghai University, Shanghai 200444, China
3. Department for Earth and Environmental Sciences, University of Manchester, Manchester, M13 9PL, UK
4. National Centre for Atmospheric Science, University of Manchester, Manchester, M13 9PL, UK
5. Guangdong Provincial Key Laboratory of Atmospheric Environment and Pollution Control, College of Environment and Energy, South China University of Technology, Guangzhou Higher Education Mega Center, Guangzhou 510006, China
6. Shanghai Academy of Environmental Sciences, Shanghai 200233, China
7. State of Environmental Protection Key Laboratory of the Formation and Prevention of Urban Air Complex, Shanghai, 200233, China
8. School of Energy and Environment, Southeast University, Nanjing 211189, China
9. Meteorological Development and Planning Institute of China Meteorological Administration, Beijing, 100081, China
10. Department of Advanced Technologies in Medicine & Dentistry, University "G.d'Annunzio" of Chieti-Pescara, Chieti 66100, Italy
11. Center for Advanced Studies and Technology-CAST, Chieti 66100, Italy
12. Department of Science, University "G.d'Annunzio" of Chieti-Pescara, Chieti 66100, Italy

*Corresponding author: Wang, Junfeng (wangjunfeng@nuist.edu.cn); Aruffo, Eleonora (eleonora.aruffo@unich.it)

The supplemental materials have 8 pages, 1 supporting texts, 7 figures, and 2 tables:

Text S1 HPLC separation setup, UHPLC-Orbitrap MS data analysis and quantification

Figure S1 The map of Myanmar sampling location

Text S1 HPLC separation setup, UHPLC-Orbitrap MS data analysis and quantification

1. Setting for UHPLC separation

A Waters Acquity HSS T3 column (1.8 μm, 100 × 2.1 mm) was used to fulfill the seperation with mixed mobile phase of (A) 0.1% formic acid solution and (B) 0.1% formic acid and acetonitrile. The gradient elution program was as follows: it started with 99% of A and 1% of B for 2 minutes, followed by a linear gradient to 100% of B over the next 11 minutes, continued with 100% of B for 2 minutes, then returned to 1% of B in 0.1 minutes, and maintained 1% of B for 6.9 minutes. The flow rate of the A and B mixtures was 300 μL min-1 (Wang et al., 2017).

2. UHPLC-Orbitrap MS data analysis

Non-target analysis was performed using the software MZmine 2.39 to analyze the UHPLC-Orbitrap MS data. This software provides essential functions for MS data processing, including raw data import, peak detection, shoulder peak filtering,

chromatogram deconvolution, and peak identification (Hu et al., 2016; Katajamaa et al., 2006; Pluskal et al., 2010). The detailed processing steps and parameter settings can be found in the previously published articles (Fuller et al., 2012; Kind and Fiehn, 2007; Lin et al., 2012a; Lin et al., 2012b; Wang et al., 2016). The determined molecular formulas are expressed as CxHyOzNmSn, where x, y, z, m, and n correspond to the number of C, H, O, N, and S atoms in the molecular formula, respectively. Molecular formula determination is primarily based on the detected m/z values, with a tolerance of 2 ppm in both ESI+/- modes. The detected compounds in the ambient samples were compared with those in the blank samples, and only the compounds with a sample/blank peak area ratio of $\geqslant$10 were retained.

To obtain more reasonable molecular formulas, the following specific rules were applied (Koch and Dittmar, 2006): (1) Atom counts: 1-40 for 12C, 1-100 for 1H, 0-40 for 16O, 0-5 for 14N, 0-2 for 32S; (2) Element ratios: in ESI- mode, 0.3-3.0 H/C, 0-3 O/C, 0-0.5 N/C, 0-2.0 S/C; in ESI+ mode, 0.3-3.0 H/C, 0-1.2 O/C, 0-1.0 N/C, 0-0.8 S/C; (3) Double-Bond Equivalent (DBE value, calculated as 1+(2C-H+N)/2): ranges from 0 to 25.

3. Semi-quantification of the detected organic compounds

In this study, the peak areas of detected organic compounds were semi-quantified using 3-nitrophenol (3-NP) as an external standard, with estimated concentrations reported in ng m^{-3}. It is important to note that different organic compounds exhibit varying ionization efficiencies in mass spectrometry, introducing inherent uncertainties when comparing peak areas across different molecular species. To enable relative comparisons between samples, we assumed a uniform mass spectrometric response factor for all detected compounds.

For calibration, a standard solution of 3-NP (m/z 138) at 1000 ppb in acetonitrile was analyzed in ESI- mode (**Fig. S2**). A linear calibration curve (y = 893,319x, R^2 = 0.999) was established using a dilution series of 3-NP (5, 10, 30, 50, 100, 500, and 1000 ppb; **Fig. S3**).

Figure S1 The map of Myanmar sampling location

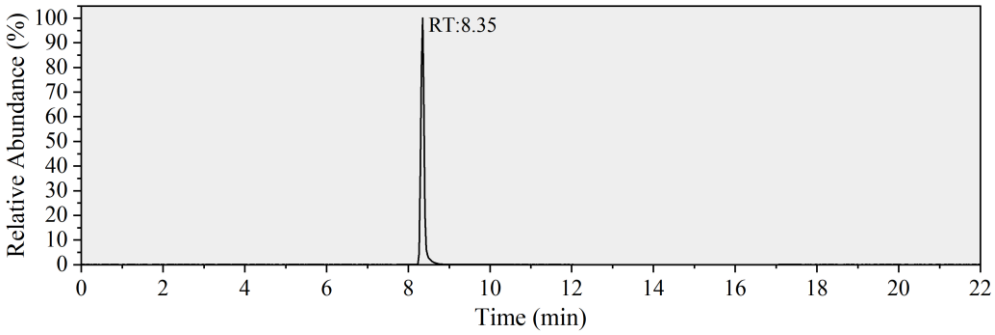

Figure S2 Chromatographic peaks of 3-NP standard substance in ESI- mode in Myanmar

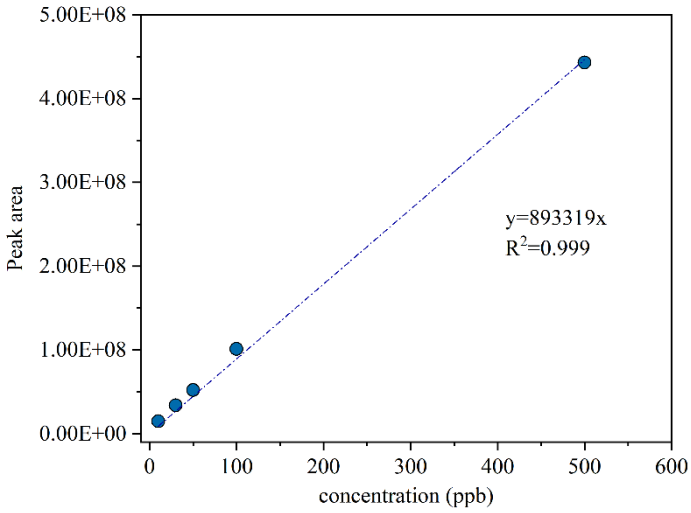

Figure S3 Calibration curve of 3-NP in acetonitrile

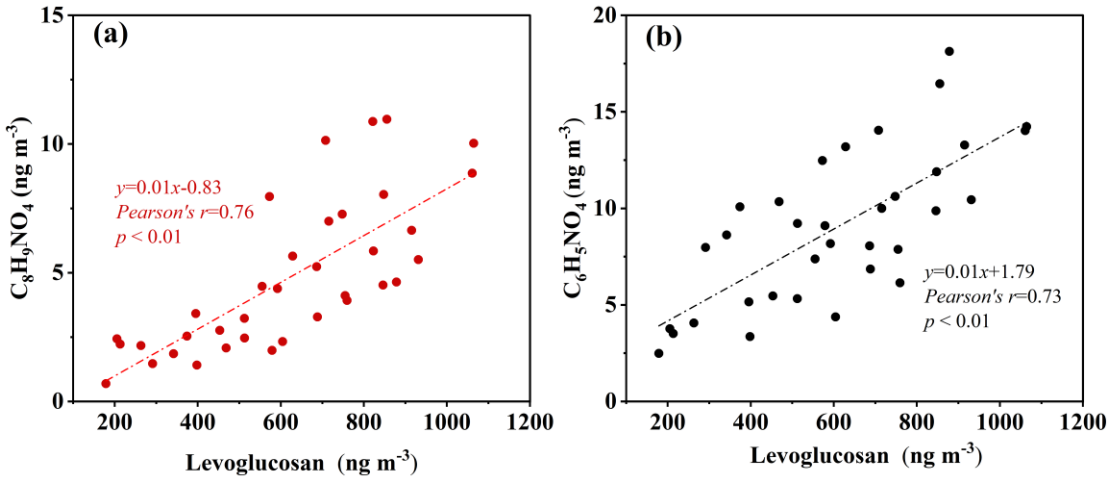

Figure S4 The correlation between $C_8H_9NO_4$ (a), $C_6H_5NO_4$ (b) and levoglucosan. Color bar is the range of RH.

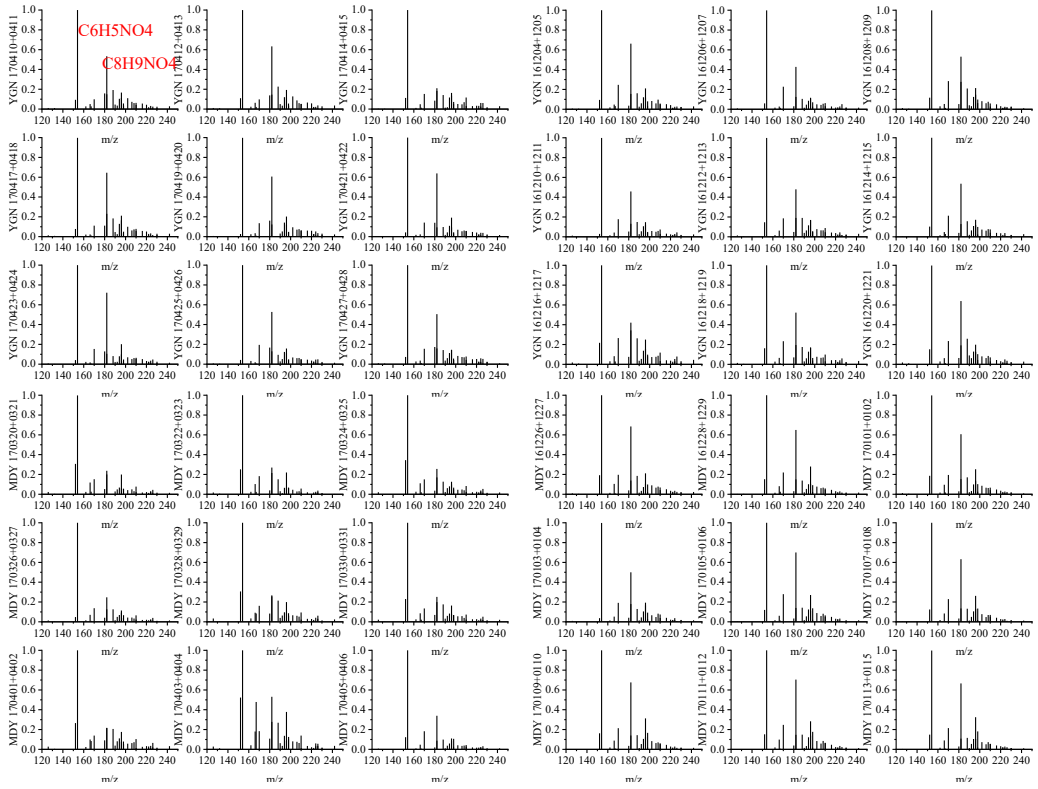

Figure S5 Mass spectra reconstructions of CHON same peaks from extracted ion chromatograms in ESI- mode. The vertical axis represents the semi-quantitative normalized concentration for each compound.

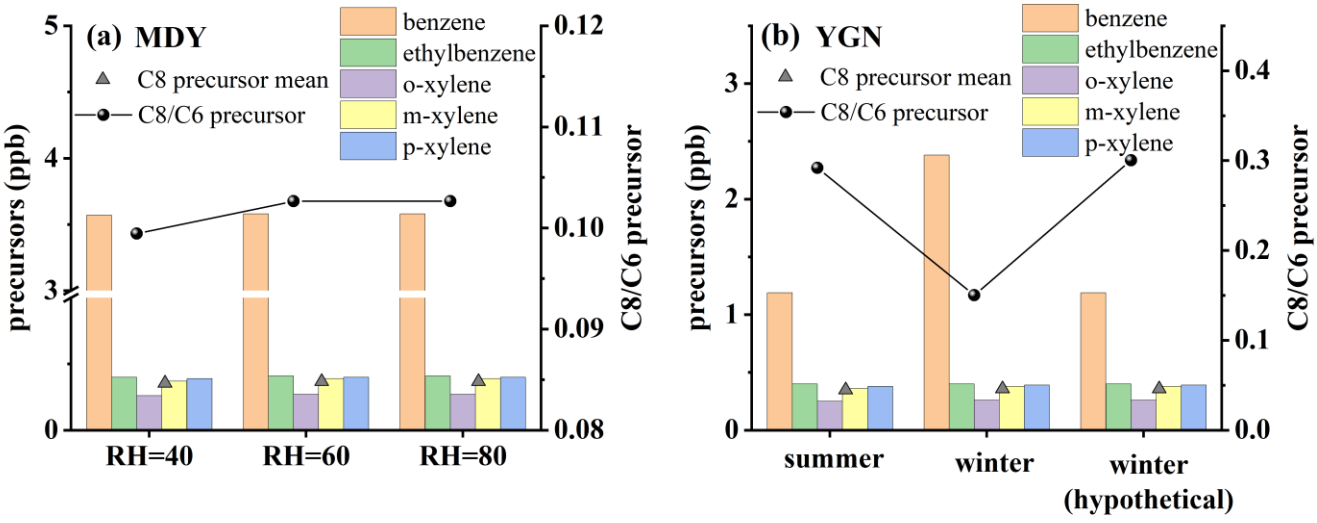

Figure S6 Distributions of simulated precursor mass concentrations for $C_8H_9NO_4$ and $C_6H_5NO_4$ under different RH conditions. In the model, the precursors of $C_8H_9NO_4$ include ethylbenzene, o-xylene, m-xylene, and p-xylene, whereas benzene is the sole precursor of $C_6H_5NO_4$. Triangles denote the average precursor concentration of $C_8H_9NO_4$.

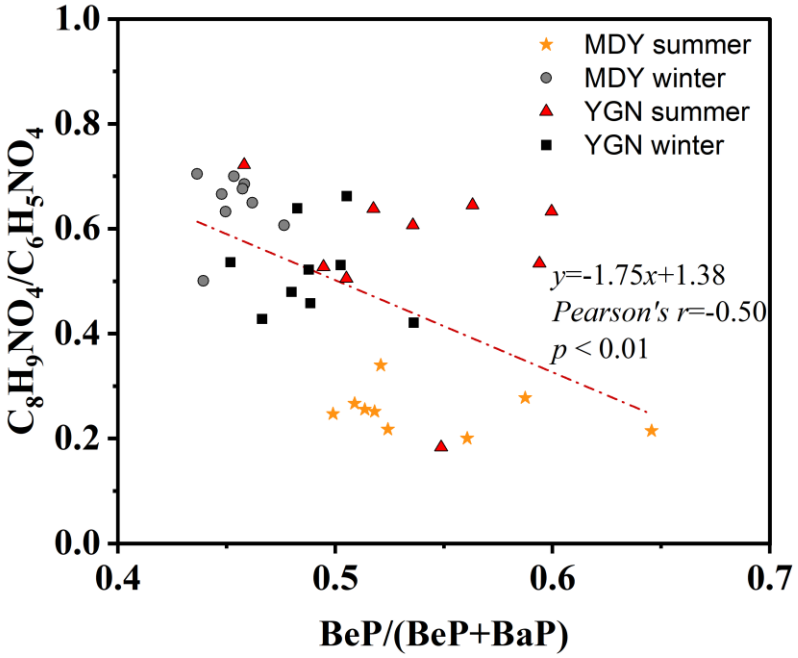

Figure S7 The correlation between BeP/(BeP+BaP) and $C_8H_9NO_4/C_6H_5NO_4$.

Table S1 The average number, peak area and corresponding compound species of different types of molecular formulas in Myanmar

Ion mode	subgroup	number	Percentage (%)	Mass concentration (ng m^{-3})	Mass concentration Percentage (%)
ESI-	CHO-	520	54.4	164.3	58.8
	CHON-	166	16.9	62.3	22.3
	CHOS-	195	19.6	43.8	15.7
	CHONS-	73	7.0	6.8	2.4
	CHNS-	19	1.9	2.3	0.8
	CHN-	2	0.2	0.2	0.1

Table S2 Summary of the number, concentration, and ratio parameters of compounds in different subgroups of $PM_{2.5}$ in Yangon and Mandalay during the winter and summer seasons.

Sample ID	Subgroup	Number of compounds	Mass concentration (ng m^{-3})
YGN-Summer	Total	772	196.8

Sample ID	Subgroup	Number of compounds	Mass concentration (ng m^{-3})
	CHO	473	127.4
	CHON	139	44.2
	CHOS	117	20.9
	CHONS	31	2.2
	CHN	1	0.1
	CHNS	11	2.0
YGN-Winter	Total	938	241.4
	CHO	507	148.5
	CHON	154	43.7
	CHOS	191	41.6
	CHONS	67	5.7
	CHN	1	0.0
	CHNS	18	1.8
MDY-Summer	Total	1064	342.7
	CHO	558	197.2
	CHON	198	84.3
	CHOS	201	49.1
	CHONS	83	9.4
	CHN	2	0.1
	CHNS	22	2.5
MDY-Winter	Total	1125	337.8
	CHO	544	184.2
	CHON	172	76.9
	CHOS	269	63.6
	CHONS	109	9.9
	CHN	3	0.4
	CHNS	27	2.7

Reference:

Fuller, S. J., Zhao, Y., Cliff, S. S., Wexler, A. S., and Kalberer, M.: Direct surface analysis of time-resolved aerosol impactor samples with ultrahigh-resolution mass spectrometry, Anal. Chem., 84, 9858-9864, https://doi.org/10.1021/ac3020615, 2012.

Hu, M., Krauss, M., Brack, W., and Schulze, T.: Optimization of LC-Orbitrap-HRMS acquisition and MZmine 2 data processing for nontarget screening of environmental samples using design of

experiments, Anal. Bioanal. Chem., 408, 7905-7915, https://doi.org/10.1007/s00216-016-9919-8, 2016.

Katajamaa, M., Miettinen, J., and Oresic, M.: MZmine: toolbox for processing and visualization of mass spectrometry based molecular profile data, Bioinformatics, 22, 634-636, https://doi.org/10.1093/bioinformatics/btk039, 2006.

Kind, T. and Fiehn, O.: Seven Golden Rules for heuristic filtering of molecular formulas obtained by accurate mass spectrometry, BMC Bioinf., 8, 105, https://doi.org/10.1186/1471-2105-8-105, 2007.

Koch, B. P. and Dittmar, T.: From mass to structure: An aromaticity index for high-resolution mass data of natural organic matter, Rapid Commun. Mass Spectrom., 20, 926-932, https://doi.org/10.1002/rcm.2386, 2006.

Lin, P., Rincon, A. G., Kalberer, M., and Yu, J. Z.: Elemental composition of HULIS in the Pearl River Delta Region, China: results inferred from positive and negative electrospray high resolution mass spectrometric data, Environ. Sci. Technol., 46, 7454-7462, https://doi.org/10.1021/es300285d, 2012a.

Lin, P., Yu, J. Z., Engling, G., and Kalberer, M.: Organosulfates in humic-like substance fraction isolated from aerosols at seven locations in East Asia: a study by ultra-high-resolution mass spectrometry, Environ. Sci. Technol., 46, 13118-13127, https://doi.org/10.1021/es303570v, 2012b.

Pluskal, T., Castillo, S., Villar-Briones, A., and Orešič, M.: MZmine 2: Modular framework for processing, visualizing, and analyzing mass spectrometry-based molecular profile data, BMC Bioinf., 11, 395, https://doi.org/10.1186/1471-2105-11-395, 2010.

Wang, X., Hayeck, N., Brüggemann, M., Yao, L., Chen, H., Zhang, C., Emmelin, C., Chen, J., George, C., and Wang, L.: Chemical characteristics of organic aerosols in Shanghai: a study by ultrahigh-performance liquid chromatography coupled with orbitrap mass spectrometry, J. Geophys. Res-Atmos., 122, 11703-11722, https://doi.org/10.1002/2017JD026930Digital, 2017.

Wang, X. K., Rossignol, S., Ma, Y., Yao, L., Wang, M. Y., Chen, J. M., George, C., and Wang, L.: Molecular characterization of atmospheric particulate organosulfates in three megacities at the middle and lower reaches of the Yangtze River, Atmos. Chem. Phys., 16, 2285-2298, https://doi.org/10.5194/acp-16-2285-2016, 2016.